A Substrate-Dependent CAD Model for Ceramic Multilayer Capacitors

Balaji Lakshminarayanan, Horace C. Gordon, Jr., *Member, IEEE*, and Thomas M. Weller, *Member, IEEE*

***Abstract*—In this paper, a substrate-dependent lumped-element model for ceramic multilayer capacitors is presented. The height and dielectric constant of a substrate have a significant impact on the frequency response of a chip capacitor, and these effects cannot be treated independently from the capacitor model. Rather, the equivalent-circuit parameters in the model must be made to vary in accordance with changes in the substrate. The model presented in this paper is suitable for microstrip-mounted components, and has been applied up to 10 GHz for values from 0.5 pF to 0.47 μF, and for FR-4 substrates ranging in height from 5 to 62 mil. The modeling and extraction procedure is demonstrated for 0805- and 1206-style capacitors.**

***Index Terms*—Ceramic capacitors, high-frequency model, microwave circuits, physical structure.**

I. Introduction

THE development of accurate broad-band equivalent-circuit models for ceramic multilayer capacitors (CMCs) presents two primary challenges. The first is representing the relatively complex and often electrically large capacitor structure using a lumped-element topology. For capacitors exhibiting only a single (series) resonance in the frequency range of interest, this problem has been addressed with good success using variations of a series *RLC* configuration [1]–[5]. The second and more formidable challenge is developing a model that correctly predicts the effects of variations in the height and dielectric constant of the substrate on which the CMC is mounted. At microwave frequencies, these board-related parasitics have a pronounced effect on the CMC performance. As will be shown in this paper, it is not unusual for the primary series resonance of a capacitor to increase greater than 5× in frequency when comparing the performance on different substrate heights. Currently available capacitor models in commercial software packages offer little in terms of substrate-dependent modeling; at best, a microstrip gap capacitor is used to represent bond-pad interaction, but this effect is relatively insignificant in comparison to the types of effects demonstrated herein.

It is the goal of this paper to examine the high-frequency performance of CMCs and put forth a lumped equivalent-circuit model that accounts for the extrinsic effects in a microstrip configuration. This model has a strong physical basis to ensure scalability for different capacitor values. Furthermore, the model is developed by extraction from S-parameters measured using multiple microstrip test fixtures, to improve the prediction of substrate dependencies. To the best of the authors' knowledge, this paper represents the first detailed investigation into board-dependent aspects of CMC modeling. The accuracy of the model at high frequencies (up to 10 GHz) is important in applications that require circuit performance to be characterized at harmonics of the fundamental signal.

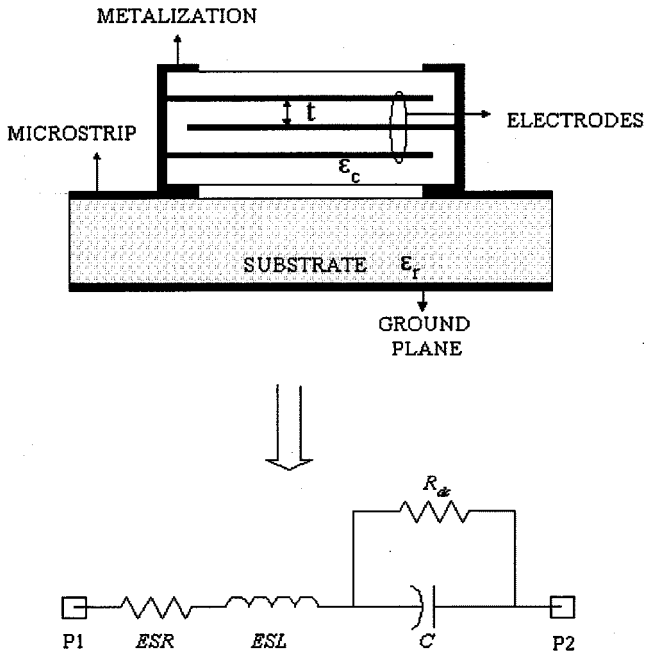

Fig. 1. Cross section of a CMC in a typical microstrip mount and an equivalent lumped-element model used for multilayer ceramic capacitors at low frequencies.

The capacitor structure under study, mounted in a microstrip configuration, is shown in Fig. 1. The capacitance is determined by the dielectric thickness between the electrodes, dielectric constant, number of electrodes, and length and width of the electrodes. In this paper, 1206- and 0805-style components are discussed, which have footprints of 3.2 × 1.6 square mm and 2.0 × 1.25 square mm, respectively. Depending on the capacitor size and manufacturer, the number of electrodes can vary from two to around 30.

In the following sections, the classical *RLC* equivalent-circuit model is described in Section II, followed by a description of the new substrate-dependent model in Section III. Expressions for circuit parameters that are used to represent higher order resonances are discussed in Section IV. After demonstrating the accuracy of the new model in Section V, an efficient technique

Manuscript received May 21, 1999.

The authors are with the Department of Electrical Engineering, University of South Florida, Tampa, FL 33620 USA.

Publisher Item Identifier S 0018-9480(00)08724-X.

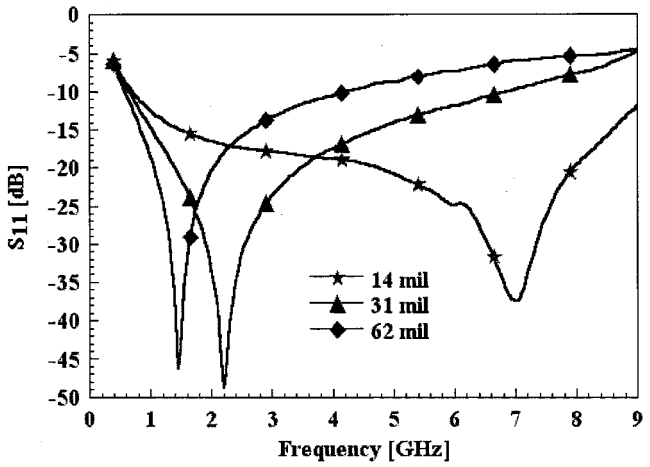

Fig. 2. S_{11} of a 1206-style 6.8-pF surface-mount capacitor measured on three different substrate thicknesses (FR-4).

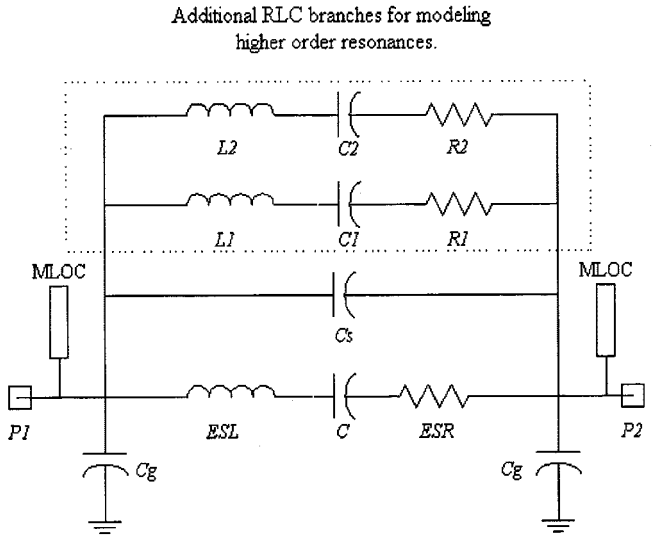

Fig. 3. Substrate-dependent model for ceramic multilayer chip capacitors.

for modeling large numbers of capacitors is described in Section VI.

Capacitor S-parameter measurements were performed using a Wiltron 360-B vector network analyzer (VNA) from 0.4 to 10 GHz, and a thru-reflect-line (TRL) calibration. Test fixtures that included the calibration standards and fixtures for mounting the components were designed for measurements using GGB 650-μm-pitch microwave probes.

II. Low-Frequency Circuit Model

A multilayer capacitor is often modeled as a series *RLC* circuit at low microwave frequencies [1]. Referring to Fig. 1, The effect series resistance (ESR) represents the resistance of electrodes and the inner electrode terminations. This resistance usually ranges from 0.01 to 1 Ω. The parasitic inductance of the inner electrodes, known as the effective series inductance, is represented by ESL and the nominal capacitance is denoted by C. An additional resistor in parallel to $C, R_{\rm dc}$ can be used to account for dielectric loss.

An important limitation of the model shown in Fig. 1 is that it does not include the effects of the microstrip ground plane. Theoretically, this model is accurate when the ground plane is located at infinity. In a practical microwave design, however, the performance of the capacitor is significantly altered by the presence of the ground. In order to demonstrate the effect, the S_{11} of a 6.8-pF 1206 capacitor on three FR-4 substrates (14-, 31-, and 62-mil thick) is given in Fig. 2. The series resonant frequency changes by a factor of 7/1.5 when comparing the performances on 14- and 62-mil substrates.

III. Substrate-Dependent Model

The topology used for the substrate-dependent model is an extension of that given in Fig. 1. Along with the addition of two equivalent-circuit parameters, closed-form expressions used to evaluate certain model parameters explicitly account for variations in the microstrip substrate height and dielectric constant.

The new model, shown in Fig. 3, is comprised of a series *RLC* circuit in combination with capacitors to ground (C_g) and a capacitance that represents the interaction between the capacitor bond pads (C_s). The parallel resistor in Fig. 1 $(R_{\rm dc})$ is discarded as it provides a direct current path from input to output, which is a potential problem when simulations are carried out using computer-aided engineering (CAE) tools such as SPICE. In order to solve the problem of having a direct current path, the capacitor C in Fig. 3 is modeled as a capacitor with a finite quality factor Q (CAPQ).[1] Assuming the conductor loss is modeled using ESR, the dielectric loss can be accounted for by the Q of the capacitor. Fig. 3 includes two *RLC* branches for modeling higher order resonances (on the top portion of the circuit), as discussed in Section IV.

The parameters for the new model are determined by treating the CMC, as shown in Fig. 4. In this figure, the model is comprised of lumped parameters (ESR, C, and C_s) and two sections of pseudomicrostrip line. The signal strip of this microstrip line represents an approximate composite of the internal electrodes of the CMC and is assumed to be located near the vertical center of the capacitor, and to have a width equal to that of the capacitor. The substrate that supports the strip is formed of two layers: the regular microstrip substrate and a layer representing the dielectric of the CMC itself. The inductance and capacitance of this pseudomicrostrip are related to the parameters ESL and C_g, as described below. The nominal capacitance C is set to the assigned value for the particular CMC. The ESR is found using a resonant line technique [7], [8] and modeled using a two-term polynomial equation. C_s is typically determined from circuit optimization, although an approximate value can be calculated from the physical dimensions of the CMC.

The parameter C_g (Figs. 3 and 4) is considered to be a combination of two capacitors in series. The first is an intrinsic capacitance (C_c) representing the capacitance from the pseudostrip to the top of microstrip substrate, and is indicated over the layer $h_{\rm CMC}$ in Fig. 4. A preliminary value for C_c can be obtained by treating the psuedostrip and the top of the substrate as a parallel-plate capacitor. However, since an approximate represen-

[1]CAPQ is available in circuit simulators such as Series IV, MDS, and ADS.

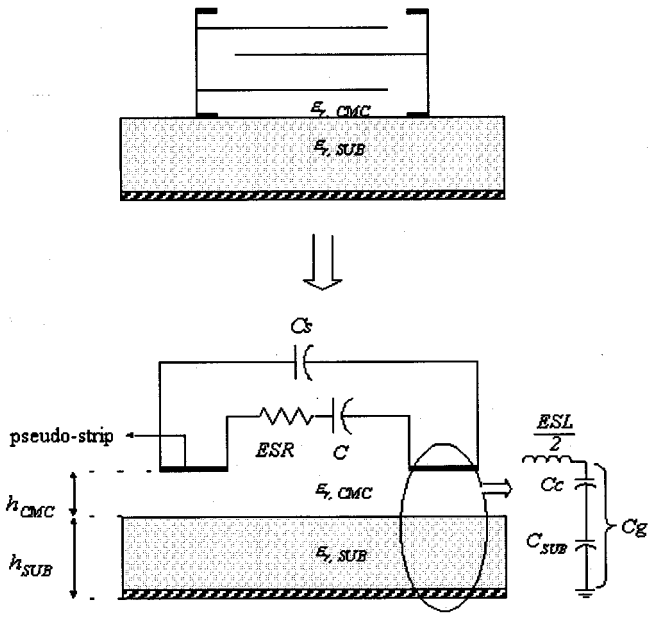

Fig. 4. Equivalent physical representation of the circuit topology. The solid lines in the lower figure represent pseudomicrostrip lines, assumed to be located near the middle of the CMC.

tation of the internal electrode geometry is being applied, the final value for C_c must be determined using circuit optimization. The second capacitor is an extrinsic capacitance $(C_{\rm SUB})$ representing the capacitance from the substrate to ground, and is shown over the layer $h_{\rm SUB}$ in Fig. 4. The capacitance $C_{\rm SUB}$ is calculated from the knowledge of the effective dielectric constant $(\varepsilon_{\rm re})$, the height of the substrate $(h_{\rm SUB})$, and the assumed width of the pseudostrip (which is equal to the capacitor width $W_{\rm cap}$) using ideal transmission-line theory. The effective dielectric constant is computed from the substrate dielectric constant using standard equations for a strip of width $W_{\rm cap}$ [12]. The equations for $C_{\rm SUB}$ [12] and C_g are given in (1) and (2), respectively, as follows:

$$C_{\rm SUB} = \left(\frac{\left(\frac{W_{\rm cap}}{h_{\rm SUB}}\right) + 1.393 + 0.667 \cdot \ln\left(\frac{W_{\rm cap}}{h_{\rm SUB}} + 1.444\right)}{120 \cdot \pi \cdot c} \right) \cdot \frac{L_{\rm cap}}{2} \cdot \varepsilon_{\rm re} \quad (1)$$

$$C_g = \frac{C_c \cdot C_{\rm SUB}}{C_c + C_{\rm SUB}} \quad (2)$$

where $L_{\rm cap}$ is the physical length of the CMC.

A dependence on substrate height is also incorporated into the equation used to evaluate the inductance of the pseudostrip (ESL). In this case, the approach has been adopted from work presented in [9]–[11], which describes the variation of the inductance of a thin strip as a function of the distance from a ground plane. The basic form of this expression is given in (3) and (4). Here, L represents the intrinsic strip inductance (with the ground at infinity), K_g is a correction factor that depends on the strip width and distance to ground, and $W_{\rm cap}$ is the width of the capacitor. The equation predicts a decrease in ESL as $h_{\rm SUB}$ decreases, leading to the increase in resonant frequency demonstrated in Fig. 2

$$ESL = L \cdot K_g \quad (3)$$

$$K_g = K_g\_a - K_g\_b \cdot \ln\left(\frac{W_{\rm cap}}{h_{\rm SUB} + h_{\rm CMC}}\right). \quad (4)$$

The coefficients K_g_a and K_g_b are determined using circuit optimization during the model extraction process.

The inductance of the capacitor also varies with frequency due to skin-depth effects, as reported in [9] and [11], and because of changes in the current distribution along the CMC bond pads. This frequency dependence is accounted for by including an additional term into the intrinsic strip inductance

$$ESL = (ESL\_a + ESL\_b \cdot f) \cdot K_g \quad (5)$$

here, f is the frequency (in gigahertz). The coefficients ESL_a and ESL_b are determined using circuit optimization.

In summary, the substrate-dependent model that accounts for the first series resonance contains six free variables (C_s, C_c, K_g_a, K_g_b, ESL_a, and ESL_b) and seven fixed parameters ($W_{\rm cap}$, $L_{\rm cap}$, $h_{\rm SUB}$, $h_{\rm CMC}$, $C_{\rm SUB}$, ESR, and ε_r), as described in Table I.

For the work described in this paper, short sections of open-circuited microstrip line were included in the model at the locations representing the solder points between the CMC and bond pads (at both ends of the circuit), as shown in Fig. 3. These lines model the effect of the bond pad that extends a short distance beneath the CMC, and their length and width are bond-pad specific. The lines introduce a small amount of additional shunt capacitance that has only a slight effect on the frequency response of the model.

IV. Higher Order Resonances

Accurate modeling of surface mount capacitors at high frequencies requires higher order resonances to be taken into account. Theoretically, n pairs of series/parallel resonances can be modeled by adding n resonant branches in parallel to the *RLC* branch. It has been found in this paper that the frequencies at which these higher order resonances occur are essentially independent of the substrate used, in strong contrast to the primary series resonance. This fact greatly reduces the computational resources that are required for model extraction. In what follows, the discussion is limited to two higher order resonant pairs, although the method could be extended as needed. This method of calculating starting values for additional elements assumes a prior knowledge of the fundamental and higher order resonant frequencies, which are experimentally determined.

The substrate dependent model (Fig. 3) is used as the starting point to derive analytical expressions for the equivalent-circuit parameters in the additional branches, which are shown inside the box of Fig. 3. In order to reduce the complexity of the resulting expressions, the ESR parameter is excluded, introducing an error of the order of 10% or less in the resulting parameter values. This step is justified in that the expressions presented below are used only as initial values to improve the rate of convergence during circuit optimization.

TABLE I
(a) PHYSICAL INTERPRETATION AND EQUATIONS WHERE FIXED VARIABLES ARE USED. (b) PHYSICAL INTERPRETATION OF THE FREE VARIABLES IN THE MODEL THAT ARE DETERMINED USING CIRCUIT OPTIMIZATION

Fixed Variables	Physical Interpretation	Use
Wcap	Width of CMC.	C_{SUB}, *Cg*, *Kg*. See Eqn.(1), (2) and (4)
Lcap	Length of CMC.	C_{SUB}, Eqn.(1)
h_{CMC}	Height of pseudo-strip to top of microstrip surface; equal to half of capacitor thickness.	*Kg*, and to obtain a approximate value for Cc
ESR	Effective series resistance.	Obtained from a resonant line technique [8]
ε_r	Dielectric constant of substrate	Eqn(1)
h_{SUB}	Height of the substrate	*Kg*, C_{SUB} Eqn (1), (4)
C_{SUB}	Capacitance from surface to ground	*Cg*, Eqn(2)

(a)

Free Variables	Physical interpretation
Cs	Interaction between bond pads and internal electrodes
Cc	Capacitance from pseudo-strip to top of microstrip substrate
Kg_a, *Kg_b*	Correction factors applied to *ESL*, for ground plane effects
ESL_a	Frequency independent effective series inductance.
ESL_b	Frequency dependent effective series inductance

(b)

The relationship between the fundamental series resonant frequency (ω_0) and an approximate strip inductance (ESL') is given in (6). The substrate-dependent parameters in this equation are C_g and ω_0; C_g is calculated using (2) and typical values range from 0.09 pF (for a 62-mil-thick FR-4 substrate) to 0.19 pF (for a 14-mil-thick FR-4 substrate). The fundamental resonant frequency (ω_0), the first higher order resonant pair (ω_1, ω_2), and the second higher order resonant pair (ω_3, ω_4) are experimentally determined by measuring the two-port S-parameters of the capacitor. C_g and ω_0 are substrate-dependent parameters, the values corresponding to a 31-mil-thick FR-4 substrates are used in (9) and (10), as this choice offers the best overall definition of all resonant frequencies among the 14-, 31-, and 62-mil-thick FR-4 boards.

Each individual LC network inside the box in Fig. 3 has a series resonant frequency at ω_2 and ω_4, which is related to $L1$, $C1$, and $L2$, $C2$, as shown in (7) and (8) as follows:

$$ESL' = \frac{(C_s + C_g + C)}{(C_s + C_g) \cdot C \cdot \omega_0^2} \tag{6}$$

$$\omega_2^2 = \frac{1}{L1 \cdot C1} \tag{7}$$

$$\omega_4^2 = \frac{1}{L2 \cdot C2}. \tag{8}$$

In order to calculate $C1$, the input impedance $(Z1_{\text{in}})$, as seen from $P1$ for the combination of the fundamental branch, and the LC network ($L1$, $C1$) is calculated. A pair of equations relating $L1$ and $C1$ is obtained using (7) and by equating $Z1_{\text{in}}$ to ∞ at the first parallel resonant frequency (ω_1). Solving these simultaneously yields the following result for $C1$:

$$C1 = \left(\frac{\omega_2^2}{\omega_1^2} - 1\right) \cdot \left[\frac{C}{1 - \omega_1^2 \cdot ESL' \cdot C} + C_g + C_s\right]. \tag{9}$$

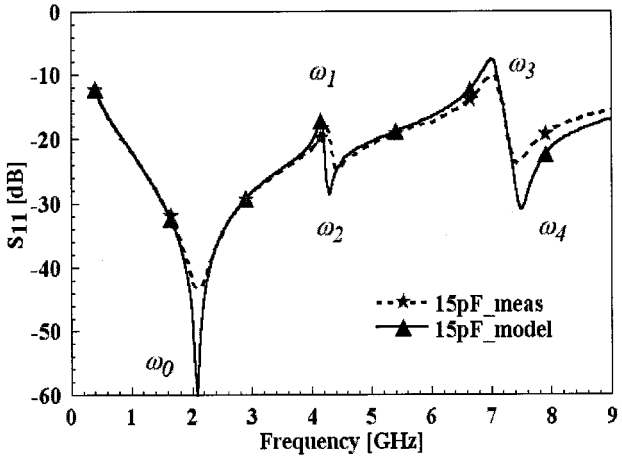

Fig. 5. S_{11} magnitude of model (solid line) and measurements (dotted line) of a 15-pF 0805–style capacitor mounted on 31-mil-thick FR-4 board showing series and higher order resonances. ω_0 is the fundamental series resonance. (ω_1, ω_3) are the first and second parallel resonances and (ω_2, ω_4) are the second and third series resonances.

The capacitor $C2$ is evaluated after deriving the expression for $Z2_{\text{in}}$, which will consist of three LC networks: an LC network for the fundamental series resonance and two LC networks for two higher order resonant pairs. Setting $Z2_{\text{in}}$ to ∞ at ω_3, and using (8), a unique value of $C2$ is obtained as follows:

$$C2 = (A + B + C_g) \cdot \left(\frac{\omega_4^2}{\omega_3^2} - 1\right). \tag{10}$$

The relationships for A and B are given in (11) and (12), respectively,

$$A = \frac{C1}{\left(1 - \omega_3^2 \cdot ESL' \cdot C\right)} \tag{11}$$

$$B = C_s + \frac{C}{\left(1 - \omega_3^2 \cdot ESL' \cdot C\right)}. \tag{12}$$

TABLE II
COMPARISON OF ELEMENTS IN THE ADDITIONAL BRANCHES ($C1$, $L1$, $R1$, $C2$, $L2$, $R2$), USING (6) AND –(12) AND THE FINAL OPTIMIZED VALUE FOR A 15-pF 0805-STYLE CMC

Elements in the additional LC branches for a 15pF 0805 style CMC	Using equation (6) through (12)	From optimization
C1 [pF]	0.019	0.019
L1 [nH]	64.544	71.995
R1 [Ω]	NA	38.458
C2 [pF]	0.027	0.0258
L2 [nH]	16.697	22.070
R2 [Ω]	NA	22.091

These expressions provide good starting values for the elements in the added resonant branches, thereby reducing the time required for the optimizer to converge to the final value.

Thus, a complete high-frequency behavior of a CMC can be described using a relatively simple model that accounts for higher order resonances. Fig. 5 shows a comparison of S_{11} magnitude of a 15-pF 0805-style capacitor mounted on 31-mil-thick FR-4 board. A comparison of calculated values using (6) and –(12) and the final optimized values for elements in additional branches ($L1$, $C1$, *and* $L2$, $C2$) is shown in Table II.

V. RESULTS

In order to demonstrate the effectiveness of the new computer-aided design (CAD) model, measured and predicted S_{11} (magnitude and phase) for a 15-pF 0805-style CMC are shown in Figs. 6 and 7. Without any loss of generality, it is intuitively clear that the other S-parameters (S_{21}, S_{12}, and S_{22}) will show a good agreement with the measured data. The results pertain to a capacitor mounted in a series two-port microstrip configuration on three different FR-4 board heights. The effective dielectric constant and the loss tangent for FR-4 are approximately equal to 3.3 and 0.022, respectively. By changing only the height of the microstrip substrate, the model is able to accurately capture the significant changes in the frequency response. The measured data shown in these figures were those used in the model extraction/optimization process.

The model was also tested on a substrate with $\varepsilon_r = 2.97$ and $h = 50$ mil, in order to verify that accurate results are obtained using substrates other than those from which the models were developed. Fig. 8 shows a plot between measured and predicted results for a 150-pF 1206-style CMC.

VI. GLOBAL MODEL

Model development for an entire family of capacitors, which may contain 60 or more individual capacitor sizes, can be accomplished efficiently using interpolation. It has been found that the free variables in the CMC model vary in a reasonably uniform manner versus capacitance value, as demonstrated in Fig. 9 for ESL_a. The solid curve in this figure was generated by interpolating between the results for 15 individual CMC models.

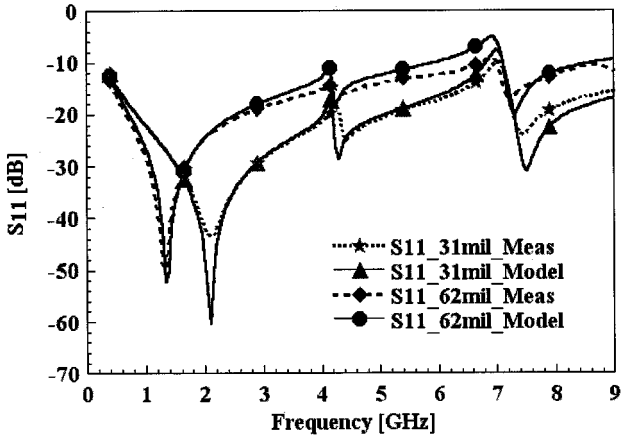

Fig. 6. S_{11} magnitude of global models (solid line) and measurements (dotted line) of a 22-pF 0805-style capacitor mounted on 31- and 62-mil-thick FR-4 boards.

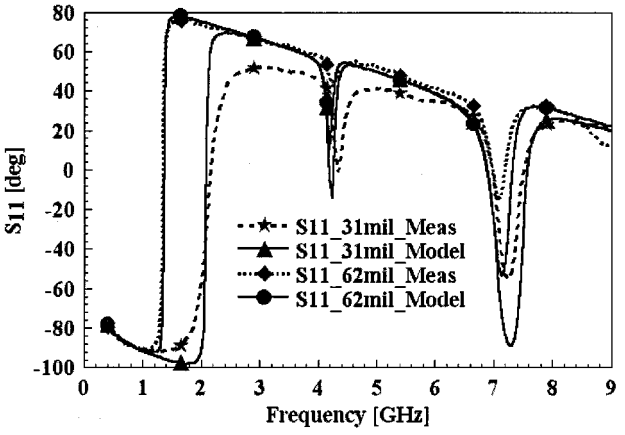

Fig. 7. S_{11} phase [in degrees] of measurements (dotted lines) and model (solid lines) for a 0805-style 15-pF CMC on 31- and 62-mil-thick FR-4 boards.

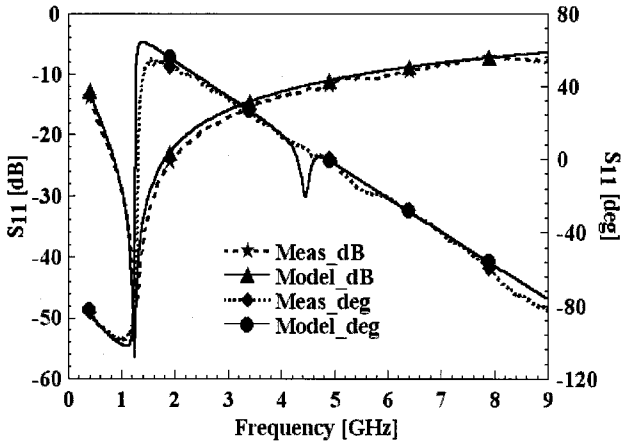

Fig. 8. S_{11} magnitude of measurements (dotted line) and model (solid line) for a 1206-style 15-pF capacitor mounted on $\mathrm{er} = 2.97$- and $h = 50$-mi-thick FR-4 board.

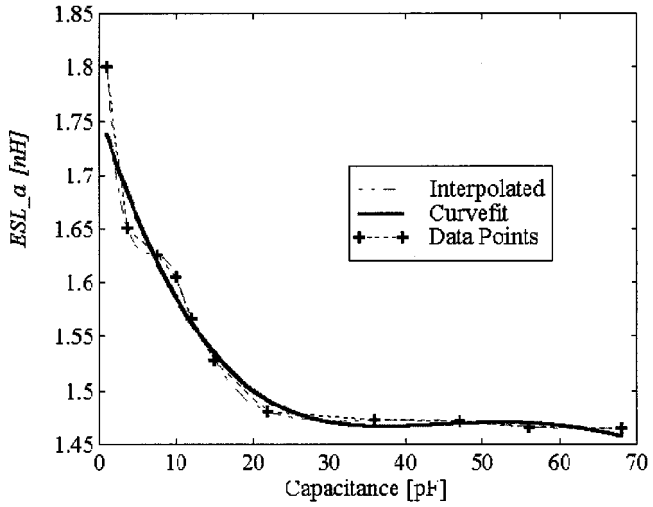

Fig. 9. Comparison between actual data points (from the model), curve fit equation, and interpolated values for ESL_a variable.

It is readily observed that parameter values for intermediate capacitor sizes can be predicted with a high degree of accuracy. The uniform variation of the parameters is a consequence of the model being closely tied to the physical properties of the CMC.

In order to facilitate CAD optimization, global CMC models have been developed in which the equivalent-circuit parameters are expressed as polynomial equations in terms of the nominal capacitance value (C). An nth-order polynomial curve fit to the interpolated values, as shown in Fig. 9, demonstrates that a single equation can be used for each parameter over the entire range of capacitor values in this particular family.

To illustrate the accuracy of the global modeling technique, one of the 15 individual CMC models was deliberately excluded during the interpolation process. Using parasitics defined by the polynomial equations, this model was regenerated and compared to the actual values. Table III gives a comparison between actual values and those obtained by interpolation.

TABLE III
COMPARISON BETWEEN CURVE FIT VALUES USING THE GLOBAL MODELING TECHNIQUE AND ACTUAL MODEL VALUES FOR A 22-pF 0805-STYLE CMC

Parameter	Actual values	Curve fit values	% Error
ESL_a [nH]	1.487	1.491	0.268
ESL_b [nH/GHz]	-0.017	-0.016	5.882
Kg_a	0.653	0.654	0.153
Kg_b	0.282	0.283	0.354
Cs [pF]	0.016	0.015	6.250
C1 [pF]	0.030	0.029	3.333
L1 [nH]	73.483	74.764	1.743
R1 [Ω]	39.430	38.426	2.546
C2 [pF]	0.052	0.050	3.846
L2 [nH]	16.399	15.945	2.768
R2 [Ω]	15.206	14.481	4.767

VII. SUMMARY

In this paper a substrate-dependent CAD model for CMCs has been proposed. The relative simplicity of the topology is convenient for extraction purposes, and critical parameters (namely, C_g and ESL) are evaluated using closed-form equations with explicit dependence on the microstrip substrate properties. Furthermore, since the model is based on an approximate physical representation of the CMC, parameter values have proven to vary in a reasonable manner with capacitor value. This uniform variation in the element values enables the global modeling technique to predict the intermediate values with a high degree of accuracy.

REFERENCES

[1] S. Yukio *et al.*, "High-frequency measurements of multilayer ceramic capacitors," *IEEE Trans. Microwave Theory Tech.*, vol. 19, pp. 7–13, Feb. 1996.
[2] A. T. Murphy and F. J. Young, "High frequency performance of capacitors," in *Proc. IEEE Electron. Comp. Conf.*, 1991, pp. 335–344.
[3] N. Coda and J. Selvaggi, "Design considerations for high-frequency ceramic chip capacitors," *IEEE Trans. Parts, Hybrids, Packag.*, vol. PHP-12, pp. 206–212, Sept. 1976.
[4] R. A. Pucel, "Design considerations for monolithic microwave circuits," *IEEE Trans. Microwave Theory Tech.*, vol. MTT-29, pp. 513–534, June 1981.
[5] L. C. N. de Vreede *et al.*, "A high-frequency model based on the physical structure of the ceramic multilayer capacitors," *IEEE Trans. Microwave Theory Tech.*, vol. 40, pp. 1584–1587, July 1992.
[6] V. K. Sadhir *et al.*, "CAD compatible accurate models of microwave lumped elements for MMIC applications," *Int. J. Microwave Millimeter-Wave Computer-Aided Eng.*, vol. 4, pp. 148–162, Apr. 1994.
[7] J. P. Maher *et al.*, "High-frequency measurements of Q-factors of ceramic chip capacitors," *IEEE Trans. Comp., Hybrids, Manufact. Technol.*, vol. CHMT-1, pp. 257–264, Sept. 1978.
[8] E. Benabe *et al.*, "Automated characterization of ceramic multi-layer capacitors," in *52nd ARFTG Conf.*, Dec. 1998, pp. 88–94.

[9] A. Gopinath and P. Silvester, "Calculation of inductance of finite-length strips and its variation with frequency," *IEEE Trans. Microwave Theory Tech.*, vol. MTT-21, pp. 380–386, June 1973.
[10] I. Bahl and P. Bhartia, *Microwave Solid State Circuit Design*. New York: Wiley, 1990.
[11] K. C. Gupta, R. Garg, and R. Chadha, *Computer-Aided Design of Microwave Circuits*. Norwood, MA: Artech House, 1981.
[12] D. M. Pozar, *Microwave Engineering*. Reading, MA: Addison-Wesley, 1993.

Balaji Lakshminarayanan received the B.S. degree in electrical and communications engineering from Birla Institute of Technology and Sciences, Pilani, India, in 1995, the M.S. degree in electrical engineering from the University of South Florida (USF), Tampa, in 1999, and is currently working toward the Ph.D. degree in electrical engineering at USF.

His main research interests are application of microelectromechanical system (MEMS) techniques for microwaves, micromachining applications for microwave and millimeter-wave circuits, and electromagnetic (EM) modeling. His research interests include CAD and characterization of monolithic-microwave integrated-circuit (MMIC) and very large scale integration (VLSI) interconnects using frequency- and time-domain full-wave methods.

Horace C. Gordon, **Jr.** (S'63–M'74) received the B.S.E.E. degree from the University of Florida at Gainesville, in 1964, and the M.S.E. degree from the University of South Florida, Tampa, in 1970.

From 1964 to 1971, he was associated with a subsidiary of Schlumberger Inc., where he designed components for analog telemetry systems. In 1972, he became an Adjunct Lecturer and, since 1977, has been a Full-Time Lecturer in the Department of Electrical Engineering, University of South Florida. His current interest is in the area of RF/microwave circuit theory and passive component modeling.

Mr. Gordon is a member of Phi Kappa Phi, Tau Beta Pi, and Eta Kappa Nu. He is a Registered Professional Engineer in the State of Florida.

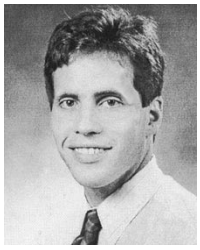

Thomas M. Weller (S'85–M'86) received the B.S., M.S., and Ph.D. degrees in electrical engineering from The University of Michigan at Ann Arbor, in 1988, 1991, and 1995, respectively.

He is currently an Assistant Professor in the Electrical Engineering Department, University of South Florida, Tampa. He has authored or co-authored over 40 papers in his field. His research involves micromachining applications for microwave and millimeter-wave circuits, packaging, electromagnetic modeling, and millimeter-wave sensors.

Dr. Weller was the recipient of the 1996 Microwave Prize presented by the IEEE Microwave Theory and Techniques Society (IEEE MTT-S).